INVESTIGATION OF SOME PROPERTIES OF MILD STEEL AT MODERATE STRAIN RATES

by

NAND SHOWKAT RAI

B. E., University of Jodhpur (India), 1964

A MASTER'S THESIS

submitted in partial fulfillment of the

requirements for the degree

MASTER OF SCIENCE

Department of Mechanical Engineering

KANSAS STATE UNIVERSITY
Manhattan, Kansas

1969

Approved by:

Major Professor

TABLE OF CONTENTS

NOMENCLATURE

ϵ = Strain (in./in.)

$\dot{\epsilon}$ = Strain rate (in./in./sec.)

σ = Stress (psi)

E = Modulus of Elasticity (psi)

Y_d = Dynamic yield stress (psi)

σ_0 = Yield Stress at absolute zero temp. (psi)

s = Density of material (lb/cu.in.)

t_y = Yield time (sec.)

t = Time (sec.)

U = Activation energy for release of dislocations.

T = Absolute temp.

N = Number of Dislocations

X,Y,Z = Rectangular Co-ordinates

M_x = Bending moment per unit length of circumference of tube (lb.in./in.)

N_ϕ = Circumferential force per unit length of tube (lb./in.)

ϕ = Angle

N_x = Axial force per unit length of circumference of tube (lb./in.)

Q_x = Shear force per unit length of circumference (lb./in.)

p = Fluid pressure (psi)

a = Original inside radius of tube (in.)

h = Wall thicness of tube (in.)

ρ = Surface density (slugs/sq.in.)

Y_s = Static yield stress (psi)

w = Displacement of tube walls (in.)

L = Half length of tube (in.)

L_e = Equivalent length of tube (in.)

r_s = Radius of small end of piston (in.)

V_p = Velocity of piston (in./sec.)

A = Orifice area (sq.in.)

ρ_f = Fluid density (lb./cu.in.)

A_p = Area of large end of piston (sq.in.)

A_s = Area of small end of piston (sq.in.)

P_g = Gas pressure (psi)

M_p = Equivalent piston and fluid weight (lb.)

P_o = Fluid pressure at yield point (psi)

$\dot{\epsilon}_o$ = Strain rate at yield point (in./in.)

CHAPTER I

INTRODUCTION

The behavior of materials under rapid loading has been the subject of many experimental investigations in the past few decades. There are two aspects involved in the response of materials to deformation under rapid loading. The first is the effect of strain rate upon the stress-strain relationship. The second aspect is the phenomenon of strain wave propagation. Impact tests and explosive loading both produce strong wave propagation effects. Strain rates produced by impact tests and explosive charges are of the order of 10^6 in. per in. per sec. The strain rates varying from 10^6 to 10^3 in. per in. per sec. have been classified as extremely high strain rates. The strain rates below 10^3 in. per in. per sec. are classified as moderate strain rates. Rates below about 0.1 in. per in. per sec. are classified as quasistatic and static strain rates.

Clark and Duwez [1]* on the basis of their previous experiments have indicated that the strain rate in impact tests varies from point to point along the specimen and for a given point it is also dependent upon the time. Therefore, the usual tension impact tests can not be employed to study the strain rate effects on the properties of a material. Thus, for investigating the influence of strain rate on properties of material, they suggested the use of thin-wall hollow cylinderical specimen in

---

* Numbers in brackets refer to references.

which only circumferential strain is induced by internal pressure varying with uniform rate. Further,it is found that at moderate strain rates,wave propagation effects may be neglected.

The program of testing materials at moderate strain rates suggested by Clark and Duwez [1] was initiated at Kansas State University. Chen [2] and Giles [3] were the first who did the preliminary work in this area. Giles built a test fixture which utilized a universal testing machine as the source of energy to drive the piston. Unfortunately,results obtained from his test fixture were not very satisfactory,and it was realized that the test fixture needed some improvements. Craft [4] in his thesis discussed some of these improvements needed,and he designed and fabricated another test fixture,keeping in view the important points which were overlooked in the previous test fixture. The author used the test fixture designed by Craft to test tubular specimen of low carbon {C-1018} steel to investigate the stress-strain relationship under different pressure loading conditions.

The purpose of this report is to present the details of experiment conducted and data obtained. Theoretical analysis of stress-strain and strain rate for thin tube subjected to impulsive pressure have been discussed. From experimental data,variation of upper yield stress and ultimate stress with strain rates has been shown.

CHAPTER II

SURVEY OF LITERATURE

The author has tried to compile in brief the work done by various researchers in the area of dynamic loading. The literature survey was completed with the help of several comprehensive studies in book form and some bibliographies.

John Hopkinson [5] was the first who attempted to investigate the influence of strain rate on physical properties of materials. In 1872, he performed experiments on steel wires by loading them with dropping weights. Further work of investigation of effects of strain rates on plain carbon steel was done by B. Hopkinson [6]. Ludwick [7], Prandtl [8], and Deutler [9] attempted to formulate the law of strain rate sensitivity. Ludwick, on empirical grounds, suggested a logarithmic law of strain rate sensitivity

$$\sigma = \sigma_o + B \log_e \dot{\epsilon} \qquad (1)$$

where B is a constant.

Prandtl and Deutler gave support to the same relationship. H. C. Mann [10] performed both tension impact and static tests and attempted to correlate the two, but without definite results. The effect of strain rate on the yield stresses was investigated by Clark and Datwyler [11], Brown and Vincent [12], Clark [13], Clark and Wood [14], Baron [15], Campbell and Duby [16], Campbell [17], Krafft and Sullivan [18], and Taylor and Malvern [19].

Clark and Datwyler performed the test on a few steels, non-ferrous metals and alloys at a velocity of about 11ft. per sec. From the results of experiment they found that dynamic yield strength is greater than static yield strength for the most of the materials tested.

Brown and Vincent [12] found that the strain rate sensitivity is generally more with weaker steels than with stronger ones. They also found that yield strength is more strain-rate sensitive than ultimate tensile strength. Clark and Wood [14] performed tensile tests on steels with a special rapid-load testing machine. They could apply tensile loads to a specimen at rates to within 5 mill. seconds. The phenomenon of delayed yield was investigated and it was shown that the delay time depends upon the yield stress.

Baron [15] conducted tensile testing on various metals, e. g. mild steel, copper, lead and aluminium, at strain rates up to 200 in. per in. per sec., and he obtained stress-strain curves at various strain rates. He found that strain rate has a definite effect on yield strength of mild steel, steel alloys, aluminium and copper, but lead is practically not affected. He discussed his results, taking into account metallurgical effects due to high strain rates.

Campbell [17] developed a relationship between yield stress and strain rate. His analysis was based on the Theory of Dislocation of Cottrell and Bilby [20].

Taylor and Malvern [19] investigated the effect of dynamic rate of strain and low temperature on lower and upper yield

stress of mild steel. They compared their results of dynamic lower yield stress of normalized steel with unnormalized mild steel at room temperature. It appears that there was no correlation. They indicated that the value of dynamic lower yield stress should be determined from the dynamic properties of unyielded material rather than those of plastically deformed material.

Manjoine and Nadai [22] observed combined effects of strain rate and temperature on steel and copper.

It is observed that strong wave effects are generated at the high loadings associated with high strain rates. The theory of plastic wave propagation was given by Von Karman [23]. The Von Karman Theory of the propagation of plastic strain waves is based on the equation ;

$$s\left(\frac{\partial^2 u}{\partial t^2}\right) = \frac{\partial \sigma_x}{\partial x} \qquad (2)$$

This is the equation of motion of an infinitesimal element of a long thin rod, u is the displacement of a particle, σ_x is direct stress in x direction. Von Karman employed a simplifying approximation that the plastic stress-strain relationship was independent of strain rate. According to this assumption the relationship between stress-strain is given by

$$\sigma_x = \sigma(\epsilon) \qquad (3)$$

$\sigma(\epsilon)$ is the stress-strain relationship in tension. From equation (3) he showed that the velocity of wave propagation is given by

$$V = \sqrt{\frac{1}{s}\left(\frac{\partial \sigma}{\partial \epsilon}\right)} \qquad (4)$$

The Von Karman theory predicted the existence of a critical impact velocity.

Clark and Wood [14] experimentally determined the critical impact velocity and concluded that critical velocity is not a specific material property, but it is a product of strain wave propagation phenomenon.

Refinements in the theory of Von Karman were mainly due to Malvern [24]. The strain rate law proposed by Malvern is somewhat similar to the law suggested by Ludwick [7], Prandtl [8] and Deutler [9]. Malvern expressed his in the form :

$$\sigma = f(\epsilon) + a \log_e(1 + b \dot{\epsilon}_p) \qquad (5)$$

Where a and b are physical parameters. Equation (5) may be rewritten as

$$\epsilon_p = \frac{1}{b} \text{ Exp } [(\sigma - f)/a] - 1 \qquad (6)$$

In his treatment of theory of plastic wave propagation, he considered equation (6) as

$$E\dot{\epsilon}_p = g(\sigma, \epsilon) \qquad (7)$$

He also obtained an expression for the rate of change of elastic strain with time :

$$E \frac{d\epsilon_e}{dt} = \frac{d\sigma}{dt}$$

$$E\dot{\epsilon} = \dot{\sigma} + g(\sigma, \epsilon) \qquad (8)$$

He used a very simple form for function:

$$g(\sigma, \epsilon) = k\,[\sigma - f(\epsilon)] \tag{9}$$

where k is multiplicative constant. His analysis was found to be most realistic. Simmons, Hauser and Dorn [25], in their theory of plastic deformation under impulsive loading, have discussed the defects in two popular theories of plastic-wave propagation, proposed by Van Karman and Malvern. According to them, the assumption of the Von Karman Theory that under dynamic conditions of stressing within the plastic range the flow stress is exclusively determined by the plastic strain, is not correct. They concluded on the basis of their experimental results that the simplifying assumption of a functional dependence of stress on strain alone leads to some discrepancies with actual observation. According to them the Malvern Theory is the better approximation. But, they believe that Malvern's assumptions concerning the behavior of materials under rapid loading are somewhat imperfect.

Sternglass and Stuart [26] also investigated the wave propagation phenomenon in copper. They performed experiments on copper strips satically preloaded into plastic region. From experimental data they concluded that even in the plastic range the velocity of stress front was the ordinary elastic wave velocity and that all stress levels were propagated at a velocity much greater than the velocity obtained by slope of stress-strain curve to which material was subjected. Similar results were reported by Riparbelli [27] on copper.

Turpow and Rippeŕger [23] investigated strain rate effects on stress-strain characteristics of aluminium and copper, and they obtained suitable data required for applying the Malvern strain rate theory to studies of plastic wave propagation.

Clark and Duwez [1] explained the inability of impact tests to reveal the true influence of strain rate on the tensile properties of the materials. They first attempted to find the stress-strain relationship of material at various strain rates by using tubular specimen subjected to internal pressure. They could obtain strain rates up to 200 in. per in. per sec. and found that the ultimate strength of material increases with increasing rate of strain up to a rate of 100 in. per in. per sec. and then is not affected appreciably.

After Clark and Duwez, rapid bursting of tubular specimen was conducted by Randall and Ginsburgh [29]. Randall and Ginsburgh used the shock tube testing machine. The pressure inside the tube was produced by igniting the fuel. The yield stress was calculated from:

$$\sigma_y = \frac{pa}{h}(1 - B) \tag{10}$$

Where a is the original inside radius and B is the negative root obtained from:

$$B^2 - B\left(A\frac{2Eh}{pa^2}\right) - 1 = 0 \tag{11}$$

A = permanent change of tube radius.

The stress before yielding was calculated as a function of time as given by:

$$\sigma = \frac{pa}{h}\left[1 - \cos\frac{t}{a}\left(\frac{\rho E}{\xi}\right)^{1/2}\right] \tag{12}$$

The strain up to yield point was obtained by:

$$\epsilon = \frac{pa}{Eh}\left[1 - \cos\frac{t}{a}\left(\frac{\rho E}{\xi}\right)^{1/2}\right] \tag{13}$$

The strain rate at the initiation of yielding:

$$\dot{\epsilon}_o = \frac{p}{Eh}\left(\frac{\rho E}{\xi}\right)^{1/2}(1 - B^2)^{1/2} \tag{14}$$

Noyes [30] described the burst tests on thin wall circular cylinder of aluminium, brass and magnesium alloys, mild steel and polymethylmethacrylate plastic. He has suggested a photo-electric shadowing system for measuring strain. Hoge [31] used thick wall tubular specimen and the Dynapak testing machine.

Since 1963, the research work in the field of dynamic loading on materials has been to investigate the stress-strain relationship on the basis of plastic wave propagation effects given by Karman [23], Malvern [24] and subsequently modified by Dorn, Hauser, and Simmons [25]. The study of dynamic plasticity is a recent introduction in this field which involves considerable mathematical techniques to obtain the stress-strain relationship.

CHAPTER III

EFFECTS OF STRAIN RATE LOADING ON PROPERTIES OF MILD STEEL

From the experimental results obtained by various researchers who have investigated the properties of materials under high strain rates, it is apparent that the resistance of materials under high strain rates differs from their resistance to static strains. The following fundamental phenomena have been discovered for mild steel under rapidly varying strains;

a. The dynamic moduli of mild steel differs only slightly from its static value. But there is marked change in relationship between plastic stress and strain. Some empirical relationships between stress, strain and strain rates have been developed. D. L. McLellan, et. al.,[32] has given a general equation which describes stress-strain relationship for various structual materials up to strain rates of 10^3 in./in./sec. including both metallic and non-metallic types. It has the form :

$$= \sigma/c\dot{\epsilon}^d + a\dot{\epsilon}^b \sigma^n \qquad (1)$$

The constants a, b, c and d are determined empirically from test data. If the dynamic moduli remains constant, equation (1) reduces to :

$$= \sigma/E + a\dot{\epsilon}^b \sigma^n \qquad (2)$$

b. The elastic limit (yield point) increases with rate of strain. This was primarily investigated by Clark and Wood [14],

Baron [15], Campbell and Duby [16], Campbell [17], and Kraft and Sullivan [18]. Campbell gave a quantitative relationship between yield stress and rate of strains.

Analysis of Campbell is based on the theory of yielding developed by Cottrell and Bilby [20]. According to them, yielding would occur when the quantity:

$$S = \frac{dt}{d\sigma} \exp \left\{ - U (\sigma/\sigma_o)/kT \right\}$$

reached some characteristic value. k is Boltzman's constant. The quantity S is proportional to $\frac{dN}{d\sigma}$. On the basis of the above argument, Campbell has given power relationships between yield stress and strain rate and between yield stress and time to yield, at constant temperature. These relationships are, at constant strain-rate tests;

$$Y_d = \sigma_o \left[(\alpha + 1) C E \dot{\epsilon}/\sigma_o \right]^{1/(\alpha+1)} \qquad (3)$$

$$t_y = (\alpha + 1) C (Y_d/\sigma_o)^{-\alpha} \qquad (4)$$

According to Yokobori [21], $\alpha >> 1$ hence (3) can be written as :

$$Y_d \propto (\dot{\epsilon})^{1/\alpha}$$

The details of derivation of equations (3) and (4) given by Campbell [17] are given in Appendix A.

c. The ultimate tensile stress, and in general the stress at failure, increases with increase in rate of strain. A very

detailed investigation into failure under dynamic loading was carried out by Clark and Wood [14]. They found that ultimate tensile stress of steels increased up to 55 percent, depending on the heat treatment. In certain cases they observed that it decreased from the static value when the steel was brittle.

d. When the instantaneously applied stress exceeds the yield point, yield occurs after a certain interval of time which depends on the magnitude of stress. This phenomenon is known as delayed yield. The relation between the period of delayed yield t and the applied stress σ has been expressed analytically by the equation:

$$t = t_o e^{-\sigma/\sigma_o}$$

Where t_o and σ_o are constants.

e. When the instantaneously applied stress exceeds the static ultimate stress failure occurs after a certain interval of time. This phenomenon is known as delayed failure. The time t before failure occurs at a stress (more than static ultimate stress) is given approximately by :

$$t = A_o e^{-C_1 \sigma}$$

Where A_o and C_1 are constants which depend on the material and the temperature.

f. The deformation under high pressure associated with high rates of loading produces twinning, and in general, work hardening. It is not known whether the amount of work hardening is comparable to that produced at low rates of strain.

g. There are conflicting opinions for increase or decrease of fatigue strength during fatigue test after material has been plastically deformed under high strain rates.

CHAPTER IV

STRESS, STRAIN AND STRAIN RATE RELATIONSHIP OF THIN WALL TUBE SUBJECTED TO DYNAMIC LOADING

The thin wall tube used in the experiment for the purpose of investigating the stress-strain relationship can be treated as a thin cylinder of short length simply supported at the ends, i.e. the radial motion of the walls is constrained at ends, but it is free to rotate. In analysing the behavior of such a cylindrical tube under dynamic loading, certain simplifying assumptions were made. The assumptions are outlined as follows:

1. strains produced are small compared to unity.
2. tube consists of rigid-plastic material which does not work harden.

Further analysis of the problem was done by assuming that the tube consists of elastic-plastic material, but in that case, plastic strains were assumed to be large compared to elastic strains. The thin wall tube under consideration is shown in Fig. 1.

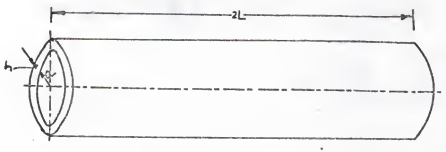

Fig. 1.

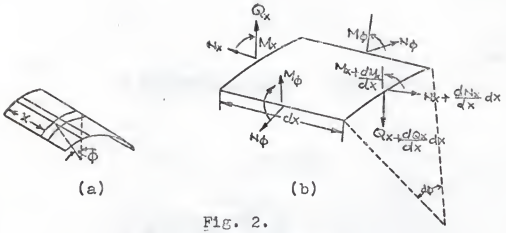

Fig. 2.

BASIC EQUATIONS

In developing the basic equation, the work of Timoshenko [33] and Hodge [34] was taken in to consideration. Fig. 2a shows the upper half of the thin wall tube under consideration. An element is cut from the tube by two adjacent generators and the two cross sections perpendicular to the x axis, and its position is defined by the coordinate x and angle ϕ.

The forces acting on sides of the element are shown in Fig. 2b. In addition, a load will be distributed below the surface of the element due to pressure p. Now, consider the equations of equilibrium which are obtained by projecting the forces on the axial and radial axes and by taking the moment of forces about the tangential axis.

$$\Sigma F_{axial} = 0$$

$$\frac{dN_x}{dx} dx \, a d\phi = 0$$

$$\Sigma F_{radial} = 0 \qquad (1)$$

$$\frac{dQ_x}{dx} dx\, ad\phi + N_\phi dx\, d\phi - pdx\, ad\phi = 0$$

$$\Sigma M_{tangential} = 0$$

$$\frac{dM_x}{dx} dx\, ad\phi - Q_x ad\phi\, dx = 0$$

M_x will be taken positive if it corresponds to tensile stresses at the inner surface, N_ϕ will be positive if it corresponds to tensile stresses at the inner surface, N_x will be positive in tension, N_x force in axial direction is constant and will be taken equal to zero to simplify the analysis.

The remaining two equations can be written in the following simplified form:

$$\frac{dQ_x}{dx} + \frac{1}{a} N_\phi = p \qquad (2)$$

$$\frac{dM_x}{dx} - Q_x = 0$$

Eliminating Q_x from these equations, the resulting equation becomes :

$$\frac{d^2 M_x}{dx^2} + \frac{1}{a} N_\phi = p \qquad (3)$$

Under suddenly applied pressure the tube walls have motion in the plastic range, and dynamic equations for tube wall forces are obtained by adding appropriate inertia terms to the static equations of equilibrium.

Thus equation (3) becomes:

$$\frac{d^2M_x}{dx^2} + \frac{1}{a} N_\phi - p - \rho \frac{d^2w}{dt^2} = 0 \qquad (4)$$

It is convenient to discuss the problem in terms of dimensionless variables defined in terms of physical constants. Dimensionless quantities are defined as:

$$n = \frac{N_\phi}{2Y_s h}, \qquad m = \frac{M_x}{Y_s h^2}$$

$$P = \frac{pa}{2Y_s h}, \qquad W = \frac{w\,a}{2Y_s h}$$

$$y = x/L, \qquad C = \frac{L}{\sqrt{ah}}$$

On substitution of dimensionless quantities in equation (4), the resulting equation becomes:

$$\frac{m''}{2C^2} + n - P - \ddot{W} = 0 \qquad (5)$$

where primes indicate differentiation with respect to y and dots with respect to t.

Solution of equation (5) in plastic range can be obtained by assuming the yield criteria. To arrive at this assumption, Hodge and Ramanoi [35] have indicated that if the state of stress (i.e. stress resultants) of the shell is plotted in two dimensional space with cartesian coordinates n, m then the condition for initial yield will appear as a closed interaction curve, and various such curves have been proposed by Drucker [36] and Hodge [37]. To simplify the analysis, a square

intersection curve will be assumed, as shown in Fig. 3.

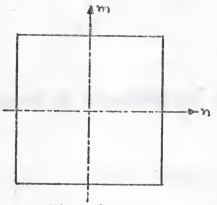

Fig. 3.

From this curve, initial condition for elasticity is obtained as:

$$-1 < n < 1, \quad -1 \leq m \leq 1$$

For thin cylinder under consideration the yield will occur when:

$$n = 1, \quad m \leq -1 \tag{6}$$

For rigid-plastic material to be in plastic region the value of n will be constant and it will be unity. The maximum value of m will be -1. Now for solving equation (5), initial and boundary conditions can be stated, as follows:

$$W(y,0) = \dot{W}(y,0) = 0 \tag{a}$$

$$W(0,t) = \dot{W}(0,t) = 0 \tag{b}$$

$$W'(1,t) = \dot{W}'(1,t) = 0 \tag{c}$$

$$m(0,t) = 0 \tag{d}$$

$$m(1,t) = m_{max} = -1 \tag{e}$$

$$m'(1,t) = 0 \tag{f}$$

Now for tube consisting of rigid plastic material, equation (5) becomes:

$$\frac{m''}{2c^2} + 1 - P - \ddot{W} = 0 \qquad (7)$$

For pressure pulse of constant magnitude P, solution to equation (8) is obtained for m and W as:

$$m = c^2\left\{(P-1)y^2 - 2(P-1)y - \left[(P-1) - \frac{1}{c^2}\right]\sin\left(\frac{\pi y}{2}\right)\right\} \qquad (9)$$

$$W = \frac{\pi^2 t^2}{16c^2}\left[c^2(P-1) - 1\right]\sin(\pi/2y)$$

The details of the solution to Equation (9) are given in Appendix B.

The above solution to equation (5) is obtained under assumptions that the tube consists of a rigid-plastic material, and pressure pulse is of constant magnitude. But, in actual condition the tube consists of elastic-plastic material and pressure is a function of time.

For elastic-plastic material it is possible to obtain the solution if stress-strain law under dynamic loading is known. In general:

$$N = 2n\sigma$$

$$\sigma = f(\epsilon, \dot{\epsilon})$$

or $$\sigma = f(W, \dot{W})$$

$$N = 2nf(W, \dot{W})$$

$$\frac{N}{2Y_s n} = \frac{1}{Y_s} f(W,\dot{W})$$

$$n = 1/Y_s \, f(W,\dot{W})$$

Substituting the value of n in equation (5), the resulting equation becomes:

$$\frac{m''}{2c^2} + 1/Y_s f(W,\dot{W}) + P - \ddot{W} = 0 \qquad (10)$$

Equation (10) can be solved if $f(W,\dot{W})$ were known, which is only possible through experimental data. Solution to equation (10) will be very useful for design of thin shells in plastic range. The solution could not be obtained due to inadequate information available about the stress-strain law under dynamic loading.

CHAPTER V

TESTING SYSTEM

To test materials at high rates of strain has been considered a difficult task, and many experimental approaches to its resolution have been made in the past. Essentially, a testing system has to fulfill three basic requirements; first, technique for obtaining rapid loading; second, means of measuring strain; and third, technique for measuring the magnitude of stress or stresses acting at the point where strain is measured. Testing systems which satisfy these requirements have been built in the past in various different ways. Clark and Duwez were first to design a testing system for testing tubular specimen at high strain rates. Based on similar principle, one such testing system used by the author designed and fabricated at KSU is shown in Fig. 4. The following discussion of the test fixture is mainly based on the report given by Craft [4].

TEST FIXTURE

The schemetic of the test fixture is shown in Fig. 5. High pressure gas from gas reservoir G acts on the large end of double ended piston P_s. This causes the piston to move against the pressure of fluids in reservoir S (acting on small end) and reservoir M. Fluid in reservoir M passes through the metering orifice to fluid reservoir by pushing plunger P. The rate of flow of fluid through the metering orifice controls the rate of pressure variation in reservoir S. The fluid in reservoir S flows

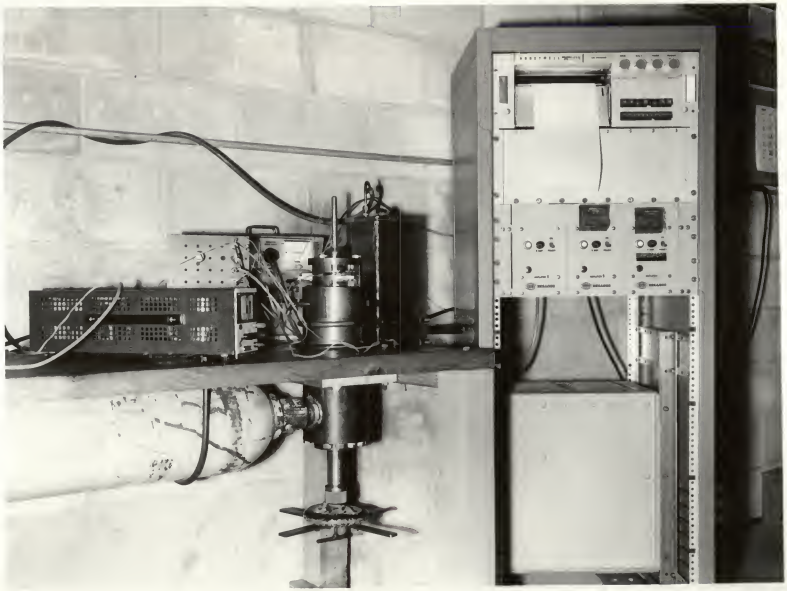

Fig. 4. Testing System

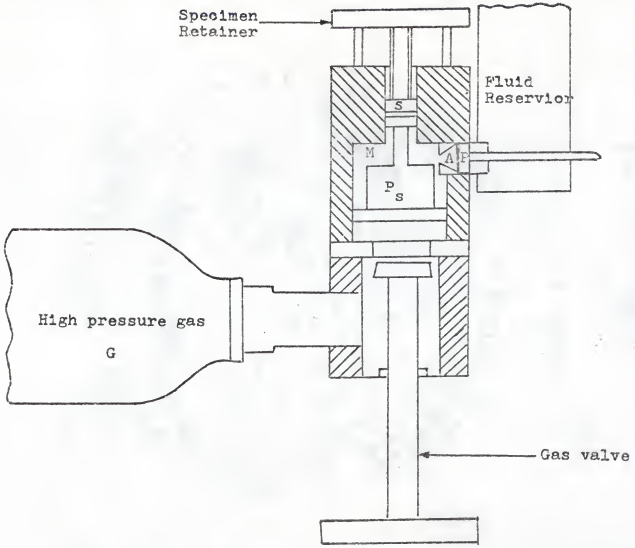

Fig. 5. Schematic diagram of test fixture

in to the specimen and deforms it.

Thus, the rate of deformation of specimen depends upon the rate at which the fluid flows from reservoir M and is controlled by the size of metering orifice. Assuming that fluids in reservoirs and in cylinder to be incompressible and expansion of specimen to be uniform, then strain rate can be computed from formula:

$$= \frac{v_p}{2L_e} \left(\frac{rs}{a}\right)^2 \tag{1}$$

Velocity of piston is given by:

$$V_p = \sqrt{\frac{2(C_v A)^2 P_g}{\rho_f A_p^2}} \quad \tanh \sqrt{\frac{f A_p^4 P_q}{2(C_v A)^2 M_p^2}}\, t \tag{2}$$

If piston velocity is assumed to be uniform, then strain rate would be uniform. The uniformity of piston velocity depends upon the pressure variation in reservoir M during test. The pressure variation in reservoir M depends upon the difference between pressure of fluid in reservoir S and pressure of gas in reservoir G and areas As and Ap. The pressure in reservoir S at any instant is given by:

$$p = \alpha_1 P_\ell - \rho_f/2\, V_p^2 \left(\frac{A_m}{AC_v}\right)^2 (\alpha_1 - 1) \tag{3}$$

The different rates of strain can be obtained by varying the size of orifice. The area of orifice is computed from:

$$A = \frac{2\,\pi L_e\, a^2\, (\alpha_1 - 1)^{3/2} \dot{\epsilon}_o}{C_v \sqrt{\frac{2}{\rho_f} P_o (n\alpha_1 - 1)}} \tag{4}$$

where :

$$\alpha_1 = \frac{A_o}{A_s}$$

Using the above formula, area of orifices for various strain rates is given in Table I.

STRESS MEASURING DEVICE

Stress measuring device is a simple transducer designed and fabricated at K.S.U. The transducer essentially measures the fluid pressure inside the specimen. From the known fluid pressure, stress can be computed by using the formula of thin shells; that is, circumferential stress:

$$\sigma = \frac{pa}{h}$$

The transducer consists of two parts threaded together. In lower part a strain gage is fixed. Lead wires from the gage pass through the hollow upper part of the transducer assembly to two terminals of one of the four arms of a wheatstone bridge. The other arms of the bridge are fixed resistances with one variable resistance required for balancing the bridge. The output of the bridge is connected to the viscorder galvanometer through an amplifier. The frequency response of the galvanometer is 1000 cps. The wiring diagram and transducer is shown in Fig. 6.

For calibrating the transducer, a dummy tube of 0.060 in. wall and $3\frac{1}{2}$ length was made and was loaded with static fluid pressure in the test fixture. The transducer was inserted in the dummy tube. For known static fluid pressure (10 times the

TABLE I. METERING ORIFICE SIZES

Strain Rate in./in./sec.	Orifice Area sq. in.	Orifice Dia in.
0.01	0.000063	0.009
0.10	0.00063	0.028
1.0	0.0063	0.089
5.0	0.0315	0.020
10.0	0.0630	0.283
15.0	0.0945	0.346
25.0	0.157	0.447
30.0	0.1890	0.495
100	0.630	0.895

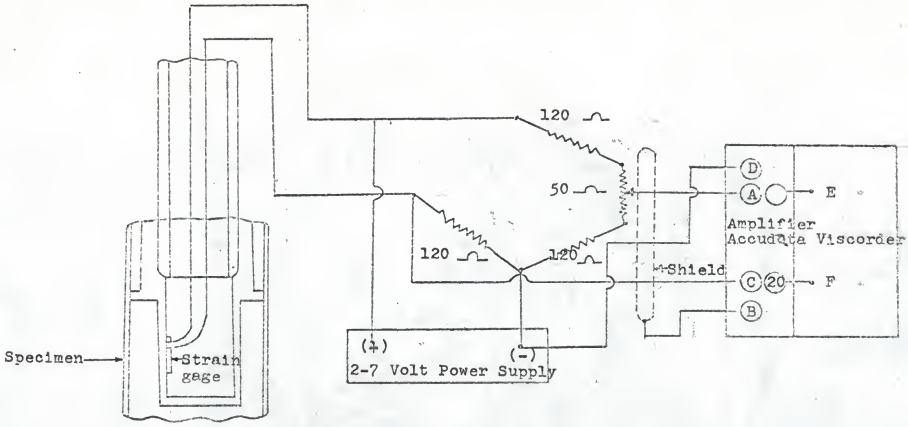

Fig. 6. Stress measuring device

pressure in gas reservoir), deflection of galvanometer light spot was recorded. Three positions of galvanometer light spot were recorded on viscorder paper for fluid pressures of 3000, 4000 and 5000 psi. The calibration curve, based on three readings, is shown in Fig. 7.

STRAIN MEASURING DEVICE

Circumferential strain on specimen was measured by three high resistance potentiometers equally spaced around the circumference of the specimen, Fig. 8. These potentiometers measure the radial displacement, w, of the specimen from which circumferential strain w/a can be calculated. The potentiometers are mounted in a metal cylinder which also acts as a shield against fluid spray upon the rupture of the specimen. Across the potentiometers, hooked in series, a current source of 6 ma (milli amperes) is applied. The output voltage from the potentiometers is amplified and recorded on a viscorder galvanometer having a frequency response of 3000 cps.

For calibration, three potentiometers were equally displaced a known distance, and corresponding deflection of galvanometer light-spot was recorded on viscorder paper. For three such displaced position of potentiometer, deflections of galvanometer light spot were obtained. From these data a calibration curve was obtained and found to be a straight line which shows the linear relationship between potentiometer displacement and galvanometer deflection, Fig. 9. From the calibration curve it is found that .007033 in. displacement of potentiometer corresponds

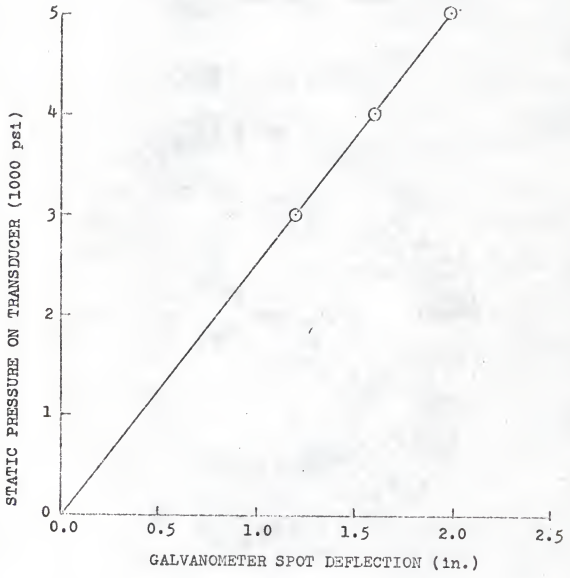

Fig. 7. Calibration curve for stress measuring device

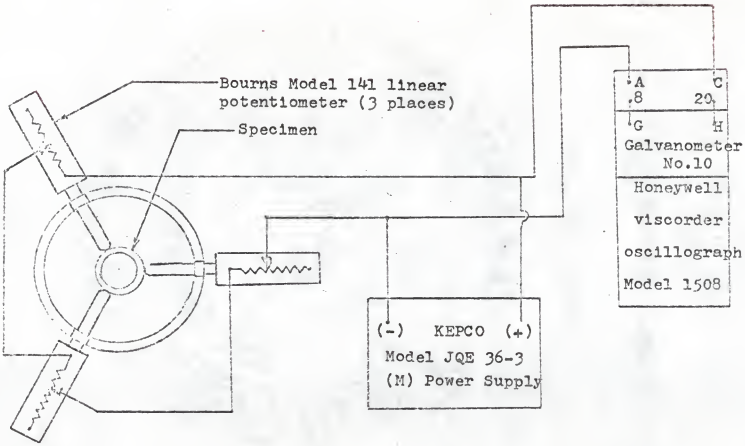

Fig. 8. Strain measuring device

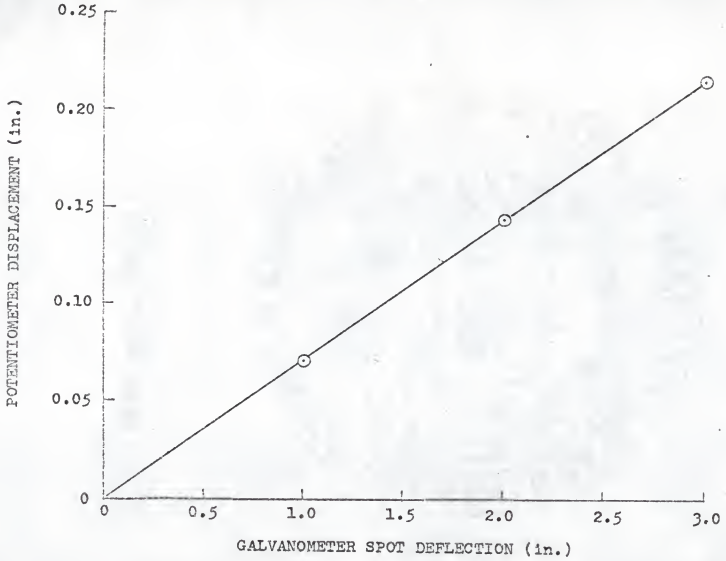

Fig. 9. Calibration curve for strain measuring device

to 0.1 in deflection of galvanometer light spot on paper.

TEST SPECIMENS

The specimen used for testing materials at high strain rates are thin wall tubes. The specimen dimensions and finish are given in appendix C. The material tested by the author was low carbon steel (C-1018) in the annealed condition. Specimen were made out of tubular stock in normalized condition. Tubular stock was turned on both inside and outside diameters and subsequently honed and polished at inner and outer surfaces, respectively. The honing and polishing on specimen were done after they were annealed. The annealing of specimen was done at a temperature of 1400 ^{o}F and were kept at this temperature for a period of about 40 minutes and then cooled slowly.

Basis of choosing a particular wall thickness was to limit the fluid pressure required for bursting the tubular specimen. The limit on fluid pressure is a very important factor in design on the test fixture. The details of specimen design are given by Craft [4]. The wall thickness is kept large to minimize the effects of tolerances and eccentricity.

CHAPTER VI

EXPERIMENTAL PROGRAM

The experimental program consists of moderate strain rate tests and static tests on tubular specimen. The details of both of these tests are given as follows:

MODERATE STRAIN RATE TEST

Experiments were performed to test the tubular specimen at various strain rates e.g., 1, 5, 10, 25, 30 in./in./sec. The procedure is broadly outlined as follows:

1. Install the required size of orifice
2. Fill the system with metering fluid
3. Reset the piston to bottom of stroke
4. Set the release mechanism
5. Install the specimen in place
6. Perform the test

The details of the procedure outlined above are given by Craft [4].

MODERATE STRAIN RATE TEST RESULTS

A typical viscorder record for tests on tubular specimen at a strain rate of 5 in./in./secs. is shown in Fig. 10. The upper trace is the displacement of specimen wall, and lower trace is the pressure of fluid inside the specimen. For a particular size of specimen and using calibration curves for pressure and displacement, viscorder records are converted into

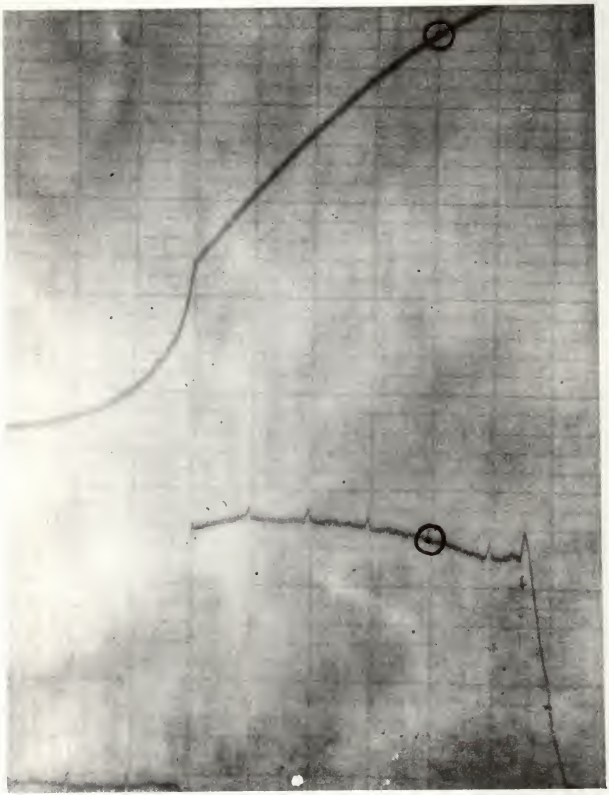

Fig. 10. Viscorder record for specimen No. 4 tested at strain rate 5 in./in./sec.

stress [pa/h] vs. time and strain [w/a] vs. time diagrams. The diagrams so obtained for all the specimen tested are given in appendix D.

The results of dynamic tests made on tubular specimens are presented in Table II. The theoretical rate of strain in the specimen has been computed according to equation (1), Chapter V and is expressed in./in./sec. The actual strain rate is comouted from the slope of the strain-time diagrams given in the appendix D. In cases where the slope of the strain time diagram is not constant, the average of slope at the beginning of plastic deformation and the point of fracture is taken to find the actual strain rate. The values of ultimate strength and yield stress have been computed from stress-time diagrams. The maximum diameter of the specimen was measured after the test. For this diameter, maximum hoop strain was computed. For purpose of discussing the conclusions of results, it was felt to take only certain typical cases which in view of author were true representation of the specimen lots tested at various strain rates. The stress-strain diagram at various strain rates for these typical cases is shown in Fig. 11. Burst specimen are shown in Fig. 12

STATIC TEST

A great difficulty was faced in performing the static test with the procedure used for testing specimen at the moderate strain rates. That was mainly due to entrapping of air bubbles in the metering fluid reservoir, which consequently increased the compressibility of the fluid.

TABLE II. STRAIN RATE TEST RESULTS

Specimen	Outside Dia. in.	Inside Dia. in.	Thickness in.	Expected Strain Rate in./in./sec.	Actual Strain in./in./sec.	Yield Stress psi	Ultimate Strength psi	Outside Dia. after Rupture in.	Maximum Uniform Strain at Rupture in./in.
1	.862	.8165	.02325	1	.79	38862	51576	1.125	.322
2	.8615	.8165	.02250	1	1.33	39690	43092	1.071	.2565
3	.862	.817	.02250	1	1.12	36304	49918	1.125	.322
4	.862	.817	.02250	5	5.26	58994	61262	1.1385	.338
5	.861	.8175	.02175	5	5.25	45804	52852	1.1330	.3327
6	.861	.81450	.02325	5	5	49263	599116	1.1510	.3560
7	.861	.817	.022	10	7.83	47340	54543	1.112	.307
8	.862	.816	.023	10	8.95	46456	54859	1.137	.337
9	.8615	.8165	.0225	10	8.95	40824	45360	1.070	.255
10	.8605	.816	.0225	10	9.395	52512	61264	1.138	.339
11	.862	.815	.02375	10	4.21	53000	67200	1.105	.299
12	.8615	.816	.02275	25	14.67	54800	62776	1.086	.274

TABLE II. (Cont'd)

Specimen	Outside Dia. in.	Inside Dia. in.	Thickness in.	Expected Strain Rate in./in./ sec.	Actual Strain in./in./ sec.	Yield Stress psi	Ultimate Strength psi	Outside Dia. after Rupture in.	Maximum Uniform Strain at Rupture in./in.
13	.861	.818	.02150	25	12.53	66584	73719	1.095	.286
14	.862	.8155	.02275	25	23.8	64960	62720	1.078	.284
15	.862	.817	.02250	25	14.33	60732	69408	1.155	.359
16	.8635	.816	.02350	30	27.8	85600	59500	1.172	.390
17	.8615	.8175	.022	30	26.125	76626	55728	1.173	.330
18	.8605	.8170	.02175	30	28.75	84400	65600	1.70	.390

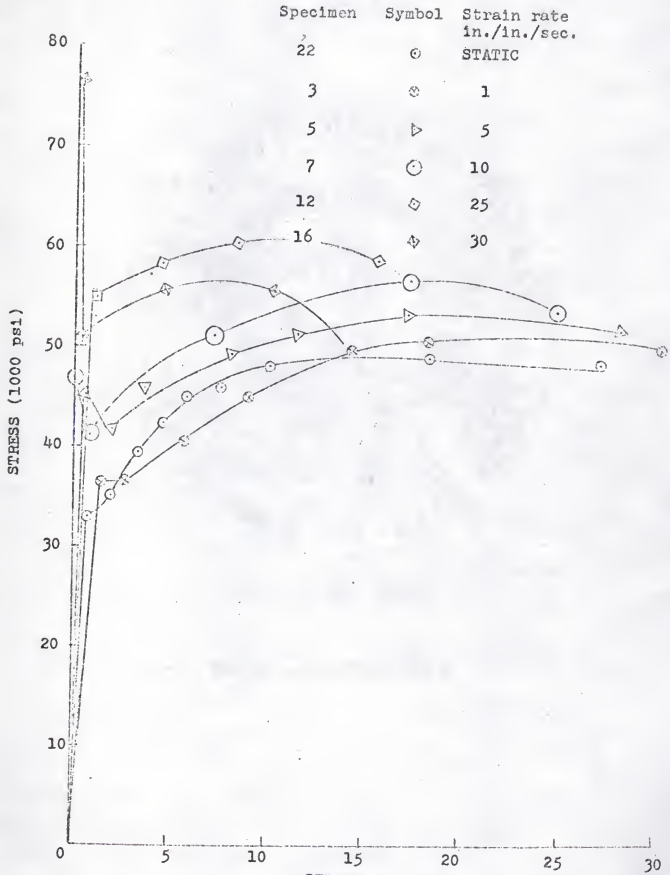

Fig. 11. Stress vs. strain diagrams for various

Fig. 12. Burst specimen tested at strain rates, from left, static, 1, 5, 10, 25 and 30 in./in./sec.

The entrapping of air bubbles in metering fluid reservoir was believed due to the small orifice through which fluid flowed to fill the metering fluid reservoir. Thus, application of gas pressure on piston caused the fluid to compress and, hence, piston raised to pressurize fluid inside the specimen without operating the release mechanism. The increase of pressure inside the specimen was enough to burst the specimen which was not desired. To avoid this difficulty a needle rod was used in the place of the release plunger, see appendix E.

STATIC TEST RESULTS

Static tests were performed on tubular specimen with the results presented in Table III. The results presented were obtained from the curves, stress vs. time and strain vs. time. The results show that strain rates of .01 to .025 in. per in. per sec. were obtained during the test which is reasonable to consider as static rate of strains. The yield stress varies between 30,2000 to 33,300 psi, and ultimate strength varies between 46,000 to 52,600 psi. This shows that there is not much scatter and results are fairly accurate.

DISCUSSION OF RESULTS

From the test results, the first thing that is observed is that the strain rate computed from strain-time diagram does not correspond to the expected strain rate computed according to Eq. (1), Chapter V, in all cases. In some cases, both of these

TABLE III. STATIC TEST RESULTS

Specimen	Outside Dia. in.	Inside Dia. in.	Thickness in.	Expected Strain in./in./sec.	Actual Strain in./in./sec.	Yield Stress psi	Ultimate Strength psi	Outside Dia. after Rupture in.	Maximum Uniform Strain at Rupture in./in.
19	.8615	.8185	.0215	static	.022	30200	46500	1.078	.205
20	.862	.818	.022	static	.026	33300	52350	1.115	.309
21	.862	.818	.022	static	.019	30200	47700	1.065	.260
22	.863	.817	.023	static	.0115	32700	48000	1.124	.322

are quite close, but in most cases there is a large difference. The apparent discrepancy can be attributed to the following reasons:

a. Fluid used is compressible.

b. Position of potentiometer may not correspond to the point where maximum strain occurs.

c. Expansion of walls is not uniform throughout the tube.

d. Piston velocity is not uniform.

e. Entrapping of air bubbles in the fluid caused increase in compressibility.

The reasons a, c and d directly contradicts the assumptions made in the derivation of equation (1), Chapter V. So the apparent discrepancy is inevitable. In order that this discrepancy is minimized, correct positioning of potentiometer is desired. It was found that potentiometer may be set at the point which is $1\frac{1}{4}$ in. away from the bottom of instrument ring. Author feels that this may not be true remedy for the error in strain measurement, due to the fact that the location of maximum diameter may vary from specimen to specimen. Another way to improve the results would be to use two sets of potentiometers instead of the one in current use. From results, it was found that the ultimate stress and yield stress were scattered from specimen to specimen for the same strain rate. The scatter cannot only be accounted for by the inaccuracy of the pressure measurements, but it may also be due to non-uniform structure of thin wall specimen. The stress-time diagrams obtained for strain rates of 30 in./in./sec. are quite misleading. This is mainly

accounted for by the measuring device which is not suitable for strain rates more than 15 in./in./sec. This is due to the fact that the galvanometer used in stress measuring device has frequency response of 1100 which is quite low for strain rate more than 15 in./in./sec. So a galvanometer of higher frequency response is recommended. In addition to that, sensitivity of stress measuring device should be increased by using preamplifier. Tektronix Type E preamplifier is suggested, which has a frequency response of 60 kc.

Results of static tests are fairly close from specimen to specimen. The ratio of dynamic to static stresses (both yield and ultimate) is plotted against strain rates for the typical cases. The curves obtained are as shown in Fig. 13. From these curves it is found that ultimate stress increases gradually with strain rate. Increase in yield stress with strain rate is very rapid. At a strain rate of 25 in./in./sec. dynamic yield stress is nearly 1.67 times that of static yield stress and dynamic ultimate stress is about 1.3 times static ultimate stress.

From this it is concluded that the mild steel is a strain-rate sensitive material which confirms the previous results of various researchers, e.g. Clark and Duwez [1], Clark [13], and Manjoine and Nadai [22]. For purpose of comparison, the experimental results of Clark obtained for SAE 1020 steel is also plotted. The curves in region of strain rate below 100 in. per in. per sec. are obtained by extrapolating the actual result curves. Such curves were drawn from experimental results of Clark by Syed [41]. It is seen that the curves for yield stress

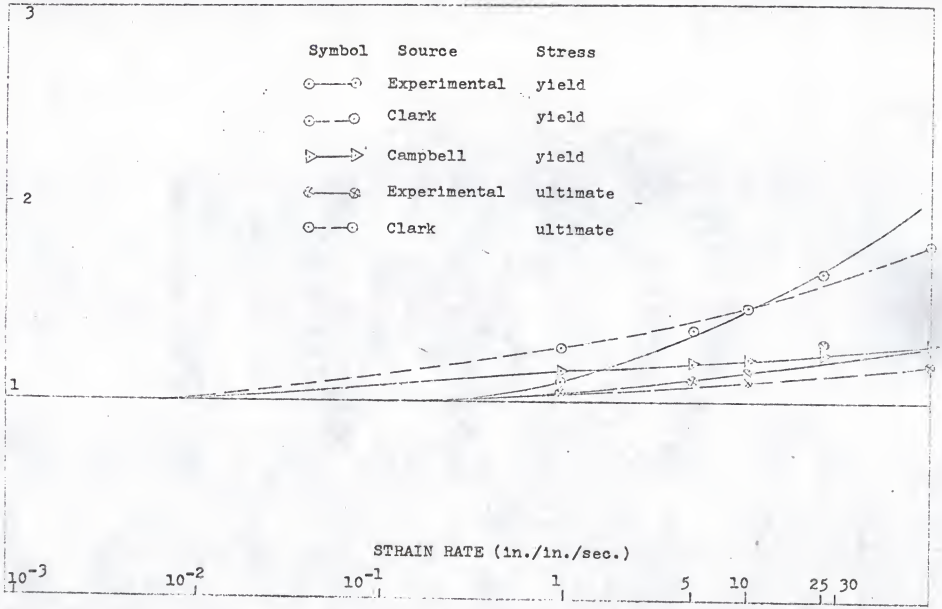

Fig. 13. Effect of strain rate on stress ratio

are scattered, where as curves for ultimate stress are quite close in two cases. A theoretical curve for yield stress is also plotted by using the following equation given by Campbell [17].

$$Y_d \propto (\dot{\epsilon})^{1/\alpha}$$

The value of $1/\alpha$ was taken as 0.022, which was assumed by Yokobari [21] for mild steel. Theoretical curve so obtained does not verify the experimental results of the author and Clark. But if the value of constant $1/\alpha$ is taken as 0.04, the values of yield stresses are quite close to theoretical values at strain rates of 5, 10 and 25 in./in./sec. According to Campbell [17] the value of $1/\alpha$ should be nearly .053 for constant strain rate tests.

Two reasons have been given for increase of yield stress with strain rates which are as follows:

a. The influence of thermal fluctuations which reduce the yield point decreases with increasing rate of strain.
b. The resistance (due to friction stress) of lattice increases with increasing velocity of dislocations.

The photograph of broken specimen shows that the fracture in all cases is longitudinal, which means that failure is due to circumferential stress.

The stress versus strain diagrams drawn for various strain rates for typical cases show that a particular law exists which

gives relationship between stress, strain and strain rate. Empirical relation between these quantities could be established, but for that it is felt that a large number of specimen should have been tested which could not be feasible due to cost and limited time available.

From strain versus time diagrams it is found that for strain rates above 10 in./in./sec., strain rate is not uniform, which according to Craft [4] was uniform. From mechanics of plastic deformation it is seen that strain rate is not uniform but is function of time. This confirms the actual results obtained. The detailed verification of analysis based on mechanics of plastic deformation could not be possible for reasons explained above.

RECOMMENDATION FOR FUTURE WORK

It is felt that further work of testing materials may initially be done on the same material which was tested by the author. The data and results obtained by author may be included in future and from these data a general empirical relationship between stress, strain, and strain rate established. Such an empirical relationship is discussed in Chapter III of this thesis. After establishing this empirical relationship further analysis of stress, strain, and strain for thin tube based on mechanics of plastic deformation may be done.

Similar work may be done on other materials, e.g. other plain carbon steels, alloy steels, aluminum and aluminum alloys.

Theoritical work may be done for investigating the stress-

strain characteristics of materials subjected to high loadings associated with high strain rates. Such types of loading produce strong plastic wave propagation effects. The wave propagation effects could be analysed mathematically with theories proposed by Dorn, Hauser, and Simmons [25].

Measurements of stress and strain plays very important roles in obtaining the reliable test results. Thus, it is felt that much emphasis should be given in improving the existing techniques, and new techniques may also be designed and developed in future.

LIST OF REFERENCES

1. Clark, D. S. and P. E. Duwez, "The Influence of Strain Rate on Some Tensile Properties of Steel." Am. Soc. of Testing Mts., Vol. 50, 1950, p. 560.

2. Chen Hsueh Hsiao, "A Fixture for Testing Materials at Medium Strain Rates." Master's Report Submitted to Dept. of Mechanical Engg., Kansas State University, 1963.

3. Giles, G. L., "Material Properties at Medium Strain Rates." Master's Report Submitted to Dept. of Mechanical Engg., Kansas State University, 1964.

4. Craft, R. L., "The Analysis and Design of a System for Testing Materials at Intermediate Strain Rates." Master's Thesis Submitted to Dept. of Mechanical Engg., Kansas State University, 1969.

5. Hopkinson, J., Collected Scientific Papers. Vol. 11, 1872 p. 316f.

6. Hopkinson, B., "The Effects of Momentary Stresses in Metals." Proceedings, Royal Soc. (London), Vol. A74, 1905, p. 498.

7. Ludwick, P., Physikalische Zeitschrift, Vol. 10, 1909, p. 411.

8. Prandtl, L., Zeitschrift fur Angewandte Mathematik und Mechanic, Vol. 8, 1928, p. 85.

9. Deutler, Physikalische Zeitschrift, Vol. 33, 1932, p. 247.

10. Mann, H. C., "The Relation Between the Tension Static and Dynamic Tests," Proc. Am. Soc. Testing Mts., Vol. 35, Part II, 1935, p. 323.

11. Clark, D. S. and G. Datwyler, "Stress-Strain Relations Under Tension Impact Loading," Proc. Am. Soc. Testing Mts., Vol. 38, Part II, 1938, p. 98.

12. Brown, A. F. C. and N. G. D. Vincent, "The Relationship Between Stress and Strain in the Tensile Impact Test." Proc. Inst. Mech. Engrs. London, Vol. 145, No. 3, 1941, p. 126.

13. Clark, D. S., "The Influence of Impact Velocity on the Tensile Characteristes of Some Aircraft Metals and Alloys," National Advisory Committee for Aeronautics Technical Note No. 868, Oct. 1942.

14. Clark, D. S. and D. S. Wood, "The Tensile Impact Porperties of Some Metals and Alloys," Trans. Am. Soc. Metals, Vol. 42, 1950, p. 50.

15. Baron, H. G., "The Effect of Strain Rate on Tensile Stress-Strain Characteristics of Metals and Some Practical Applications." Sheet Metal Industries July 1962, p. 487.

16. Campbell, J. D. and J. Dubby, "The yield Behavior of Mild Steel in Dynamic Compression." Proc. Royal Soc., Vol. 236A, 1956, p. 24.

17. Campbell, J. D., "The Dynamic Yielding of Mild Steel." Acta Metallurgica, Vol. 1, Nov. 1953, p. 708.

18. Krafft, J. M. and A. M. Sullivan, "Effect of Grain Size and Carbon Content on the Yield Delay Time of Mild Steel Transaction." Am. Soc. of Metals, 1959, 51, p. 643.

19. Taylor D. B. C. and L. E. Malvern, "Dynamic Stress and Deformation in a Mild Steel at Normal and Low Temperatures." Response of Metals at High Velocity Deformation, Inter Science Publishers 1961, p. 77.

20. Cottrell, A. H. and B. A. Bilby, "Dislocation Theory of Yielding and Strain Ageing of Iron." Proc. Phy. Soc. (London) 62A, 1949, p. 49.

21. Yokobori, T., Physics Review, Vol. 88, 1952, p. 1423.

22. Nadai, A. and M. J. Manjoine, "High Speed Tension Tests at Elevated Temperatures." Part I, Proc. Am. Soc. Testing Mts., Vol. 40, 1940, p. 822.

23. Von Karman, T., "On the Propagation of Plastic Deformation in Solids," NDRC Reports A-29 (OSRD 365) Jan. 1942.

24. Malvern, L. E., "The Propagation of Longitudinal Waves of Plastic Deformation in a Bar of Material Exhibiting a Strain Rate Effects." J. of Applied Mechanics, Vol. 18, June 1951, p. 203.

25. Dorn, J. E., F. Hauser, and J. A. Simmons, "Mathematical Theories of Plastic Deformation Under Impulsive Loading." Univeristy of California MRL Publication, Series No. 132, Issue No. 2, April, 1959.

26. Strenglass, E. F. and D. A. Stuart, "An Experimental Study of the propagation of Transient Longitudinal Deformations in Elastoplastic Media," J. of Applied Mechanics, Vol. 20, Sept., 1953, p. 427.

27. Riparbelli, C., "On the Relation Among Stress, Strain, and Strain Rate in Cu Wires Submitted to Longitudinal Impact." Proc. Soc. Expt. Stress Analysis, Vol. 14, No. 1, Sept. 1954, p. 55.

28. Turnbow J. W. and E. A. Ripperger, "Strain Rate Effects on Stress Strain Characteristics of Aluminium and Copper." Proc. Fourth Midwestern Conference on Solid Mechanics, 1959, p. 415.

29. Randall, P. N. and I. Ginsburgh, "Bursting of Tubular Specimens by Gaseous Detonation." J. of Basic Engg., Vol.82-83, 1960-1961.

30. Noyes, R. B., "Rapid Bursting of Tubular Specimen." High Speed Testing Vol. IV, InterScience Publishers May 15 & 16, 1963, p. 141.

31. Hoge, K. G., "Influence of Strain Rate on Mechanical Properties of 6061-T6, Aluminium Under Uniaxial and Biaxial States of Stress." Experimental Mechanics 2, 1965.

32. McLellan, D. L. and T. W. Eichenberger, "A Desription of Strain Rate Effects on the Compressive Behavior of Pure Aluminium." High Speed Testing Vol. VI, The Rheology of Solids, 1967, InterScience Pub, p. 135.

33. TimoshenkO, S., "Theory of Plates and Shells." Mc-Graw Hill Book Company.

34. Hodge, P. G. Jr., "Impact Pressure Loading of Rigid-Plastic Cylindrical Shells." J. of The Mechanics and Physics of Solids, Vol. 3, No. 3, April, 1955, p. 176.

35. Hodge, P. G. Jr. and F. Romano, J. of The Mech. and Phy. of Solids, Vol. 4, No. 3, May 1956, p. 145.

36. Drucker, D. C., "Limit Analysis of Cylinarical Shells Under Axially Symmetric Loadings." Proc. 1st Midwestern Conf. Solid Mech. Urbana, 1952, Engg. Expt. Sta., Univ. of Ill. p. 158-163, 1953.

37. Hodge, P. G. Jr., "The Rigid-Plastic Analysis of Symmetrically Loaded Cylindrical Shells," J. App. Mech., Vol. 21, 1954, p. 336.

38. Costello, E. deL., "Yield Strength of Steel at an Extremelly High Rate of Strain." Proc. of the Conf. on the Properties of Materials at High Rates of Strain. Inst. of Mech. Engrs., London, 1957.

39. Henriksen, E. K., I. Lieberman, J. F. Wlik and W. B. Mc Pherson, "Metallurgical Effects of Explosive Straining." Symposium on Dynamic Behavior of Materials ASTM Special Technical Publication No. 336.

40. Lyushin, I. and Lensky, "Strength of Materials." Pergaman Press 1967.

41. Syed, S., "An Evaluation of Measuring Techniques Used in High Strain Rate of Testing of Materials." A Master's Report Submitted to Dept. of Mechanical Engg., Kansas State University, 1968.

42. Wood, D. S., "Introduction." Response of Metals to High Velocity Deformation InterScience Publishers 1960, p. 1.

43. Hauser, F. E., J. A. Simmon and J. E. Dorn, "Stratin Rate Effects in Plastic Wave Propagation." Response of Metals to High Velocity Deformation. Interscience Publishers 1960, p. 93.

APPENDIX A

RELATIONSHIP BETWEEN YIELD STRESS AND STRAIN RATES

According to Cottrell and Bilby [20] yield would occur when

$$S = \left(\frac{dt}{d\sigma}\right) \exp\left\{-U\left[\frac{\sigma}{\sigma_o}\right]/KT\right\} \tag{1}$$

reached some characteristic value.

$$S = \frac{dN}{d\sigma}$$

Substituting the value of S in equation (1) we have

$$\frac{dN}{d\sigma} = \frac{dt}{d\sigma} \exp\left\{- U\left[\frac{\sigma}{\sigma_o}\right]/KT\right\}$$

$$N = \int_o^t \exp\left\{-U\left[\frac{\sigma}{\sigma_o}\right]/KT\right\} dt \tag{2}$$

It is assumed that yield will occur when a certain number of the dislocations are released. With this assumption yield will occur at a time t_y given by

$$\int_o^{t_y} \exp - U\left[\left(\frac{\sigma}{\sigma_o}\right)/KT\right]dt = C \tag{3}$$

The constant C depends on the particular steel tested.

According to Yokobori [21] activation energy U may approximately be represented by

$$U = -\frac{1}{n} \log_e\left(\frac{\sigma}{\sigma_o}\right) \tag{4}$$

Where n is constant.

In dynamic test the stress is a function of time, i. e.

$$\sigma = f(t) \tag{5}$$

Substitution of the expressions for U and σ in to equation (3) gives

$$\int_{o}^{t_y} [f(t)/\sigma_o]^{\alpha} dt = C \tag{6}$$

Where $\alpha = (nKT)^{-1}$ a dimensionless constant.

$$Y_d = f(t_y) \tag{7}$$

For the constant strain rate

$$\sigma = f(t) = E\dot{\epsilon}t \tag{8}$$

Substitution of (8) into (6) gives

$$\int_{o}^{t_y} \left(\frac{E\dot{\epsilon}t}{\sigma_o}\right)^{\alpha} dt = C$$

$$\left(\frac{E\dot{\epsilon}}{\sigma_o}\right)^{\alpha} \left(\frac{1}{\alpha+1}\right) t_y^{(\alpha+1)} = C$$

$$t_y = \left[(\alpha+1)\, C\, \left(\sigma_o \dot{\epsilon}/E\right)^{\alpha}\right]^{\frac{1}{\alpha+1}} \tag{9}$$

and hence from (7) and (8)

$$Y_d = \sigma_o \left[(\alpha+1) C E \dot{\epsilon}/\sigma_o\right]^{\frac{1}{\alpha+1}} \tag{10}$$

$$Y_d \propto \dot{\epsilon}^{\frac{1}{\alpha+1}}$$

Eliminating $\dot{\epsilon}$ between (9) and (10) gives

$$t_y = (\alpha+1)\, C\, \left(\frac{Y_d}{\sigma_o}\right)^{-\alpha} \tag{11}$$

According to Yokobori [21] exponent α at room temperature is given by

$$\alpha^{-1} = nKT = 0.022 \text{ which } \ll 1$$

Equation (10) and (11) can be approximately written as

$$Y_d \propto \dot{\epsilon}^{\frac{1}{\alpha}} \tag{12}$$

$$t_y = (\alpha+1)\, C\, (Y_d/\sigma_o)^{-\alpha} \tag{13}$$

APPENDIX B

SOLUTION OF DIFFERENTIAL EQUATION FOR THIN WALL TUBE OF RIGID-PLASTIC MATERIAL SUBJECTED TO A CONSTANT MAGNITUDE PRESSURE PULSE

The governing differential equation is

$$\frac{m''}{2c^2} + 1 - P - \ddot{W} = 0 \qquad (1)$$

with following initial and boundary conditions:

$$W(y,0) = \dot{W}(y,0) = 0 \qquad (a)$$

$$W(0,t) = \dot{W}(0,t) = 0 \qquad (b)$$

$$W'(1,t) = \dot{W}'(1,t) = 0 \qquad (c)$$

$$m(0,t) = 0 \qquad (d)$$

$$m(1,t) = m_{max} = -1 \qquad (e)$$

$$m'(1,t) = 0 \qquad (f)$$

It is known that $W = f(y,t)$

$$m = g(y)$$

Equation (1) is written as

$$\ddot{W} = \frac{m''}{2c^2} - (P-1)$$

$$\dot{W} = \int[\frac{m''}{2c^2} - (P-1)]dt + C_1$$

$$\dot{W} = [\frac{m''}{2c^2} - (P-1)]t + C_1$$

From initial condition, (a), $C_1 = 0$

$$W = \int[\frac{m''}{2c^2} - (P-1)]t \, dt + C_2$$

From initial condition $W[y,0] = 0$; $C_2 = 0$.

$$W = [\frac{m''}{2c^2} - (P-1)]t^2/2 \qquad (2)$$

Since $m = g(y)$

Then

$$\frac{m''}{2c^2} - (P-1) = G(y) \qquad (3)$$

From boundary conditions (d) and (e) it is reasonable to assume that

$$G(y) = A \sin(\frac{\pi}{2}y)$$

From this assumption Equation (3) becomes

$$\frac{m''}{2c^2} - (P-1) = A \sin(\pi/2y) \qquad (4)$$

$$\frac{m''}{2c^2} = (P-1) + A \sin(\pi/2y)$$

$$\frac{m'}{2c^2} = \int[(P-1) + A \sin(\pi/2y)]dy + A_1$$

$$\frac{m}{2c^2} = (P-1)y - A(\frac{2}{\pi}) \cos(\pi/2y) + A_1 \qquad (5)$$

From boundary condition (f)

$m'(1,t) = 0$

$A_1 = -(P-1)$

Substituting the value of A_1 in (5) results in

$$\frac{m'}{2c^2} = (P-1)y - A(\frac{2}{\pi}) \cos(\pi/2y) - (P-1) \qquad (6)$$

Integrating both sides of equation (6) we get

$$\frac{m}{2c^2} = (P-1)y^2/2 - A(\frac{2}{\pi})^2 \sin(\pi/2y) - (P-1)y + A_2 \qquad (7)$$

From boundary condition $m(0,t) = 0$

$A_2 = 0$

From condition $m(1,t) = -1$ We get

$$\frac{-1}{2c^2} = (P-1)/2 - A(2/\pi)^2 - (P-1)$$

$$A = (\frac{2}{\pi})^2 [\frac{(P-1)}{2} - \frac{1}{2c^2}]$$

Substituting the value of A in (7) we get

$$\frac{m}{2c^2} = (P-1)\frac{y}{2} - [\frac{(P-1)}{2} - \frac{1}{2c^2}]\sin(\frac{\pi}{2} y) - (P-1)y$$

$$m = c^2 \left\{ (P-1)y^2 - 2(P-1)y - [(P-1) - \frac{1}{c^2}] \sin(\frac{\pi}{2} y) \right\} \qquad (8)$$

Substituting the value of A in (4) we get

$$\frac{m''}{2c^2} - (P-1) = \left(\frac{\pi}{2}\right)^2\left[\frac{(P-1)}{2} - \frac{1}{2c^2}\right] \sin\left(\frac{\pi}{2} y\right) \qquad (9)$$

From Equations (2) and (9) we get

$$W = \frac{\pi^2}{16c^2}\left[c^2(P-1) - 1\right] \sin\left(\frac{\pi}{2} y\right)t^2 \qquad (10)$$

APPENDIX C

SPECIMEN CONFIGURATION

The following specimen configuration is as given by Craft [4].

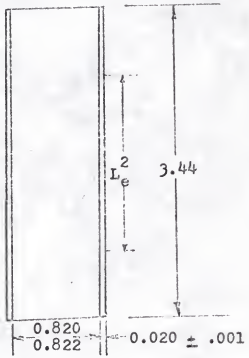

Fig. 14. Test Specimen

NOTES:

1. "Effective length (Le)" represents the actual length of specimen expected to be deformed.
2. Wall thickness variation from point to point on the specimen should be less than

3. Surface finish should be 8 to 16 RMs.
4. Dimensions are in inches.

APPENDIX D

MODERATE STRAIN RATE TEST RESULTS

Viscorder records obtained for various tests at moderate strain rates were converted into stress vs. time diagrams. These diagramd are shown in Figs. 15 to 24. For computing stress and strain from viscorder records the following precedure was used.

FOR STRESS:

Pressure at any time t is given by

$$p = d_p \times cfp$$

where

d_p = distance (in inches) of a point at time t from base line of pressure diagram (lower trace) on viscorder record.

cfp = calibration factor for pressure diagram which is equal to 2500 psi./in.

Therefore, circumferential stress at any time t is given by

$$\sigma = \frac{Pa}{h}$$

Distance d_p is measured in vertical direction.

FOR STRAIN:

Displacement of walls of tubular specimen at time t is given by

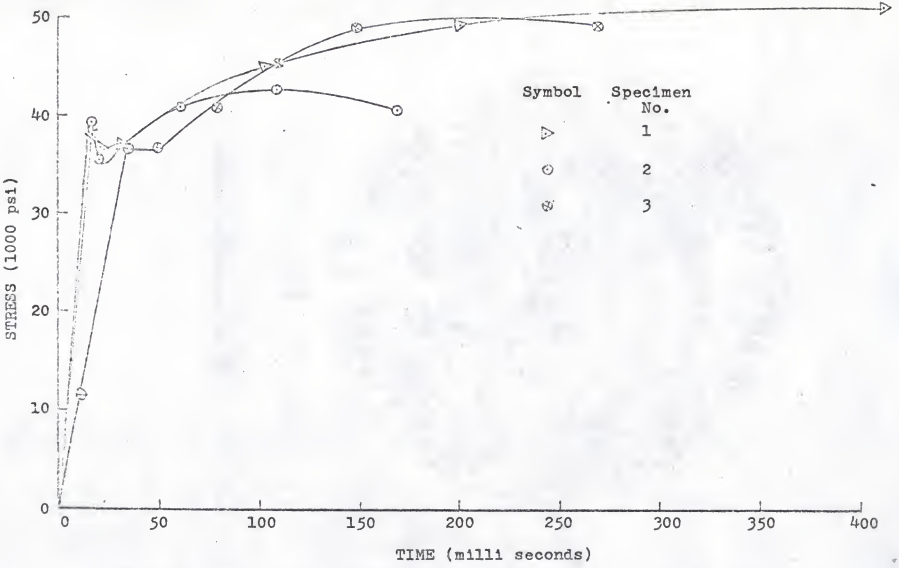

Fig. 15. Stress vs. time diagram obtained at strain rate 1 in./in./sec.

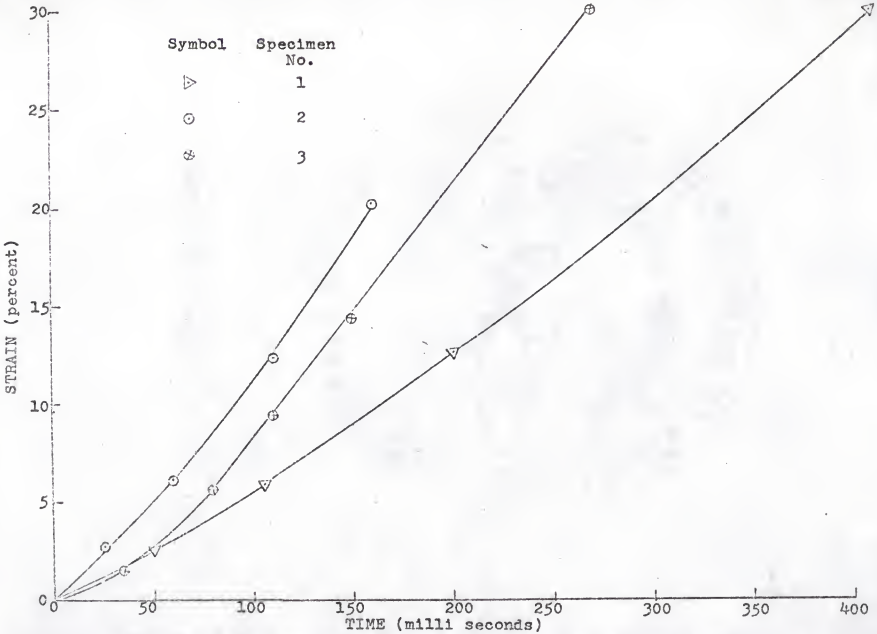

Fig. 16. Strain vs. time diagram obtained at strain rate 1 in./in./sec.

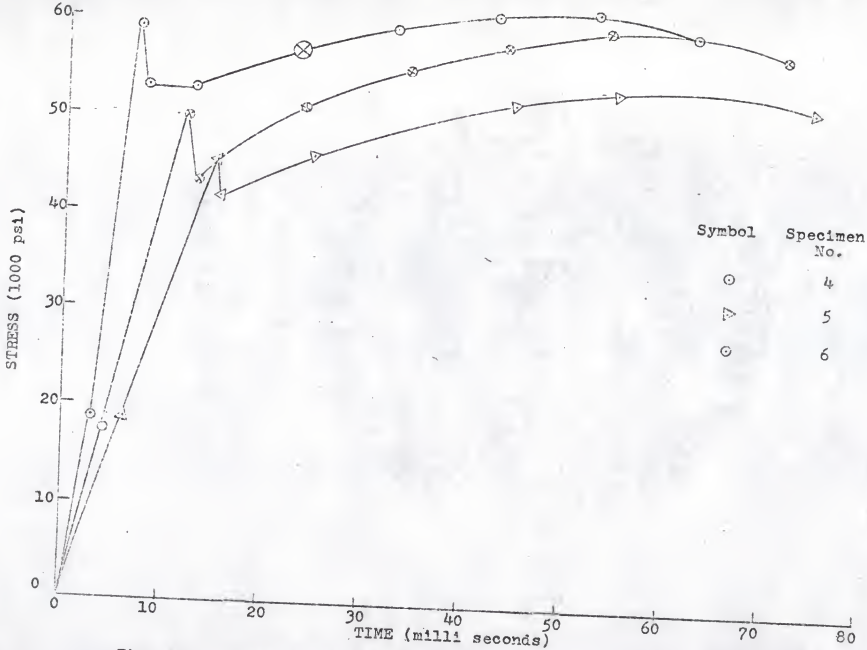

Fig. 17. Stress vs. time diagram obtained at strain rate 5 in./in./sec.

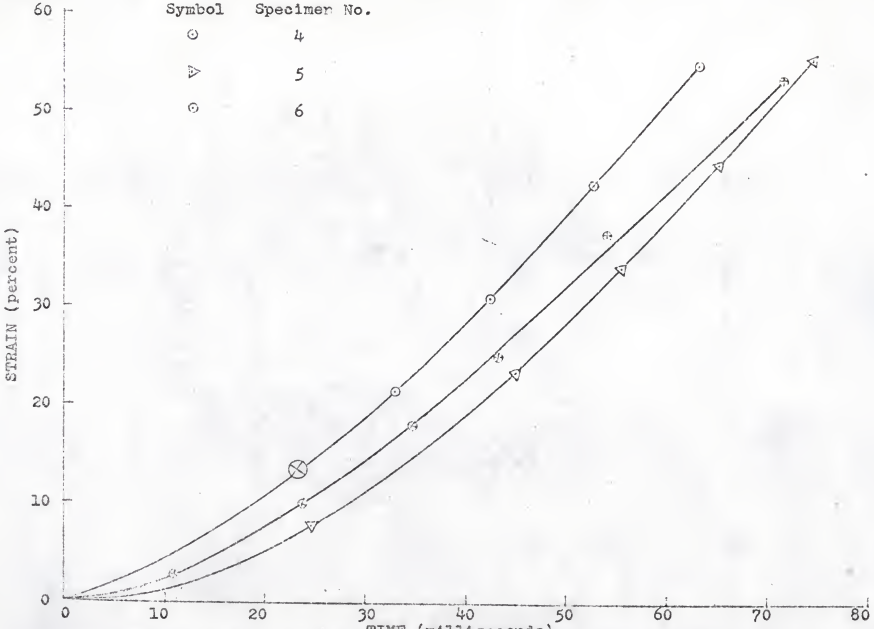

Fig. 18. Strain vs. time diagram obtained at strain rate 5 in./in./sec.

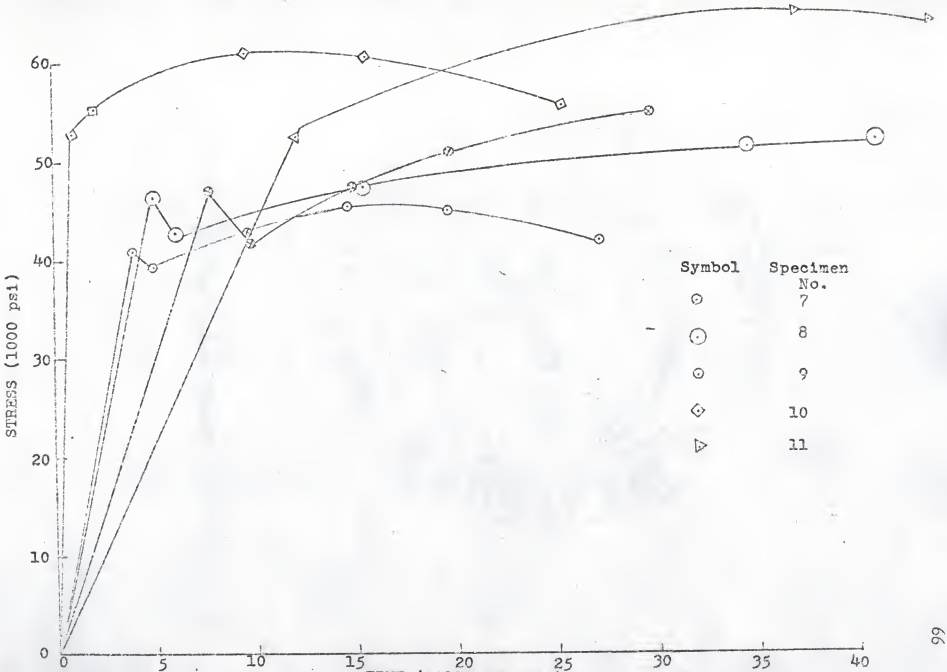

Fig. 19. Stress vs. time diagram obtained at strain rate 10 in./in./sec.

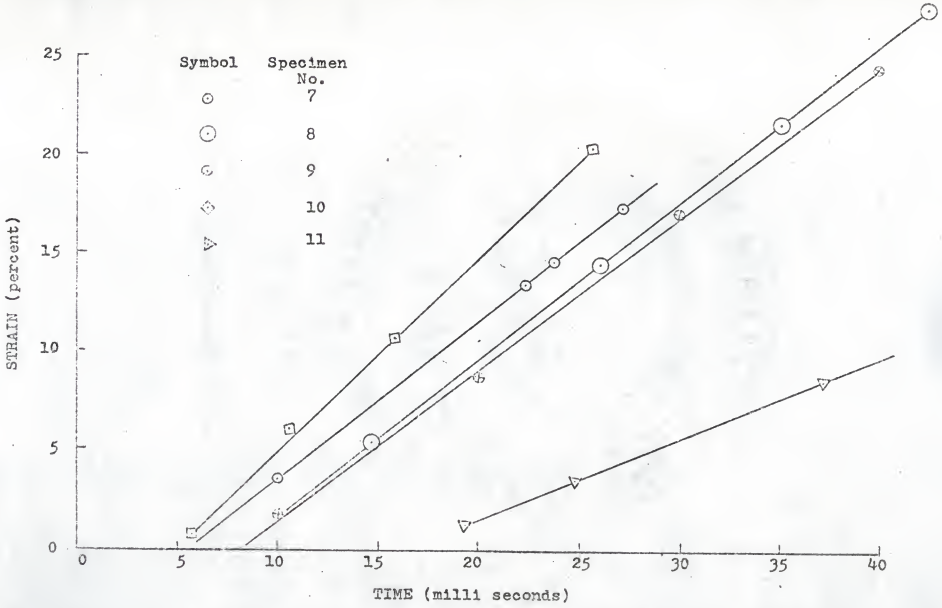

Fig. 20. Strain vs. time diagram obtained at strain rate 10 in./in./sec.

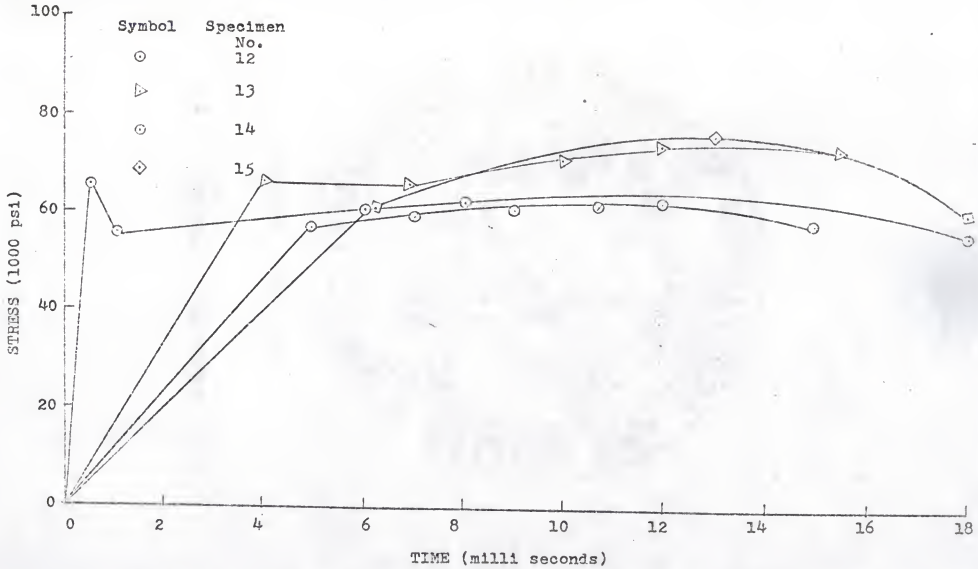

Fig. 21. Stress vs. time diagrams ontained at strain rate 25 in./in./sec.

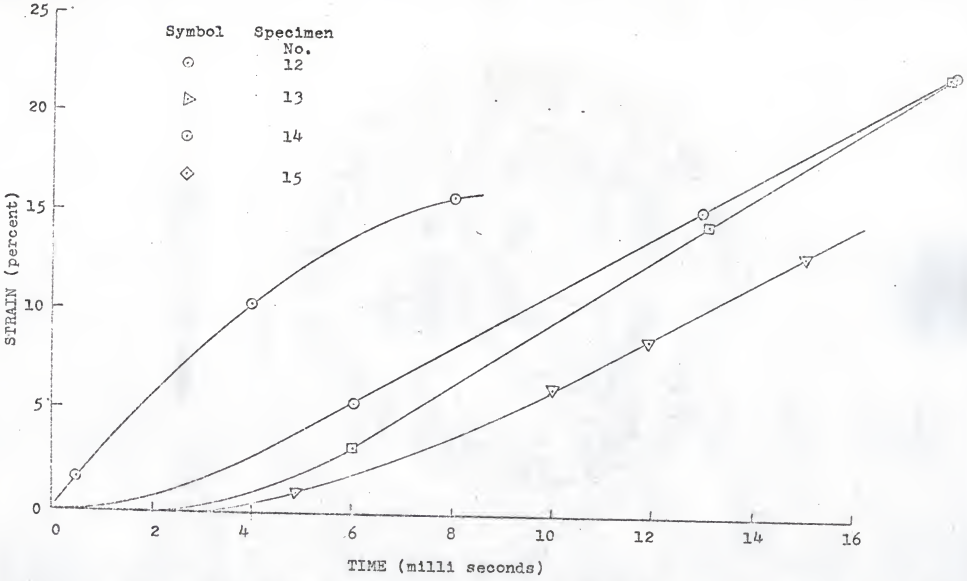

Fig. 22. Strain vs. time diagram obtained at strain rate 25 in./in./sec.

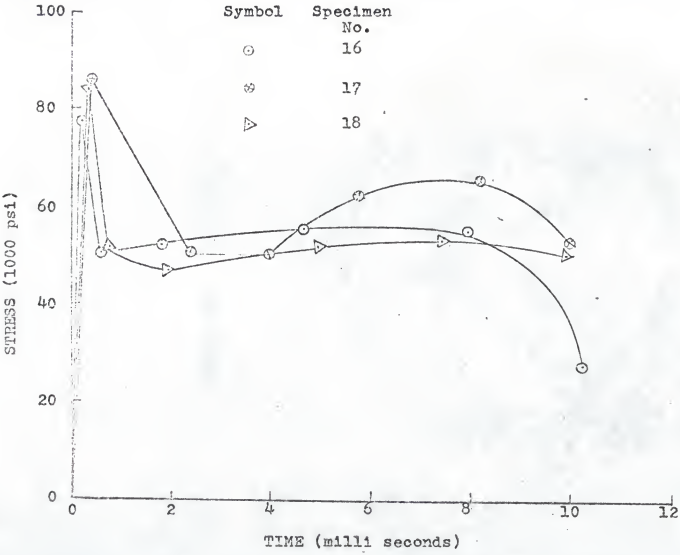

Fig. 23. Stress vs. time diagram obtained at strain rate 30 in./in./sec.

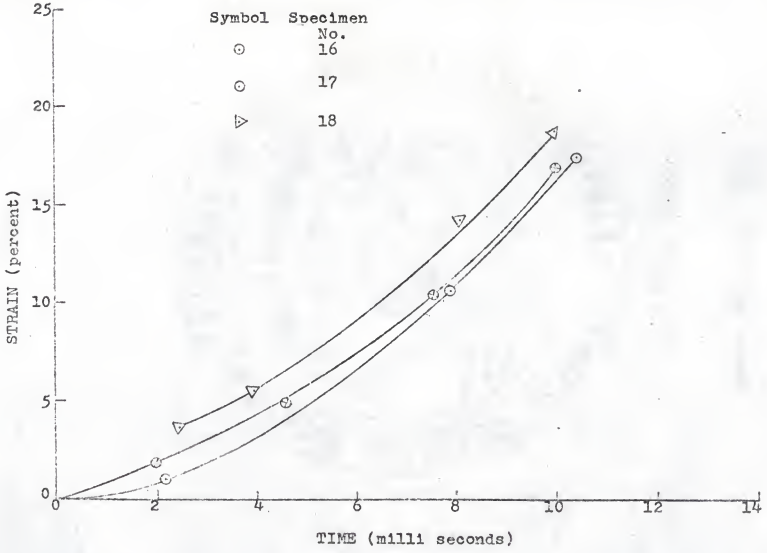

Fig. 24. Strain vs. time diagram obtained at strain rate 30 in./in./sec.

$w = d \times cfw$

where

d = distance (in inch) of a point at time t base line of displacement diagram (upper line) on viscorder record.

cfw = calibration factor for displacement which is equal to .073 in./in.

Therefore, circumferential strain at any time t is given by

$\epsilon = w/a$

Distance d is also measured in vertical direction.

Horizontal distance shows the time, and each division represents 0.01 sec.

SPECIMEN CALCULATIONS

Referring to viscorder record shown in Fig. 10 which was obtained for specimen No. 4 tested at 5 in./in./sec., the point under consideration is circled on both pressure and displacement diagrams.

Specimen dimensions are:

$a = 0.4085$ in. $\quad h = 0.0225$ in.

$d_p = 1.25$ in. (Measured from viscorder record)

$P = 1.25 \times 2500 = 3125$ lb./in^2.

$\sigma = \frac{Pa}{h} = \frac{3125 \text{ lb./in}^2. \times 0.4085 \text{ in.}}{0.0225 \text{ in.}} = 56735$ lb./in^2.

$d_w = .375$ in. (Measured from viscorder record)

$$w = .375 \text{ in.} \times .0733 \text{ in./in.}$$

$$\epsilon = w/a = \frac{.027487 \text{ in.}}{.4085 \text{ in.}} = .0678 \text{ in./in.}$$

The points are plotted on stress-time and strain-time diagrams and are shown in Figs. 17 and 18 respectively. Similar calculations were performed on various other points on the diagrams of viscorder records.

APPENDIX E

STATIC TEST ARRANGEMENTS AND RESULTS

For performing the static test a needle rod was used in the place of the release plunger. The dimensioned sketch of needle rod is shown in Fig. 25. The tapered end of the needle rod passes through the orifice of 1/3 in. dia., and it remains closed until needle rod is operated at the other end by release nut. On the other end of needle rod a small washer is brazed. The release nut is mounted on the release nipple and it is turned until inside surface of nut comes into contact with washer. The details of the arrangement are shown in Fig. 26. With this arrangement the procedure for static test is as follows:

I. To install orifice:

Follow the operating instructions 1 through 5 given by Craft (4) and then

6. Replace the needle rod for release plunger and position the needle rod so that it does not close the passage of fluid flow from reservoir through the orifice.
7. Insert 1/8 in./dia. orifice.
8. Install O-ring on orifice.
9. Install fluid reservoir.

II. Fill the system with metering fluid.

III. Reset the piston for tests.

IV. Push the needle rod till it stops moving (CAUTION--Do not

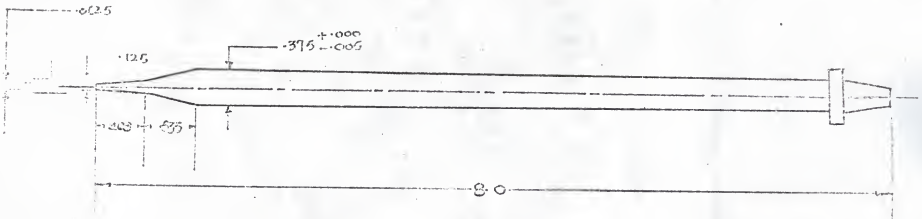

Fig. 25. Dimensioned sketch of needle rod

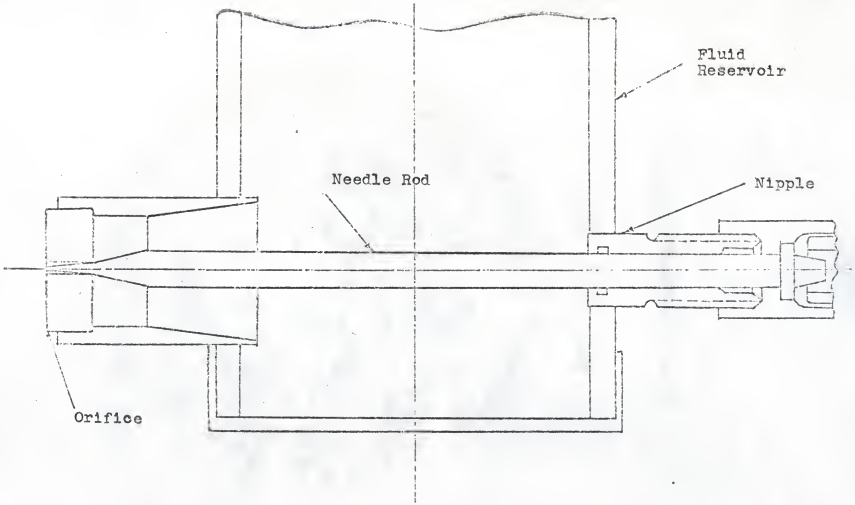

Fig. 26. Arrangements for static test using needle rod in place of release plunger

push too hard).

V. Install specimen.

VI. Initiate the test by rotating (about ½ turn) the release nut.

Note:

1. Details of operating instructions for each step is same as given by Craft [4].
2. Arrangements may be made for taking out fluid from reservoir while installing the orifice for strain rate tests.

STATIC TESTS RESULTS

Viscorder records obtained for various static tests were converted in to stress time and strain time diagram in the similar way as done for moderate strain rate tests. The diagrams are shown in Figs. 27 and 28.

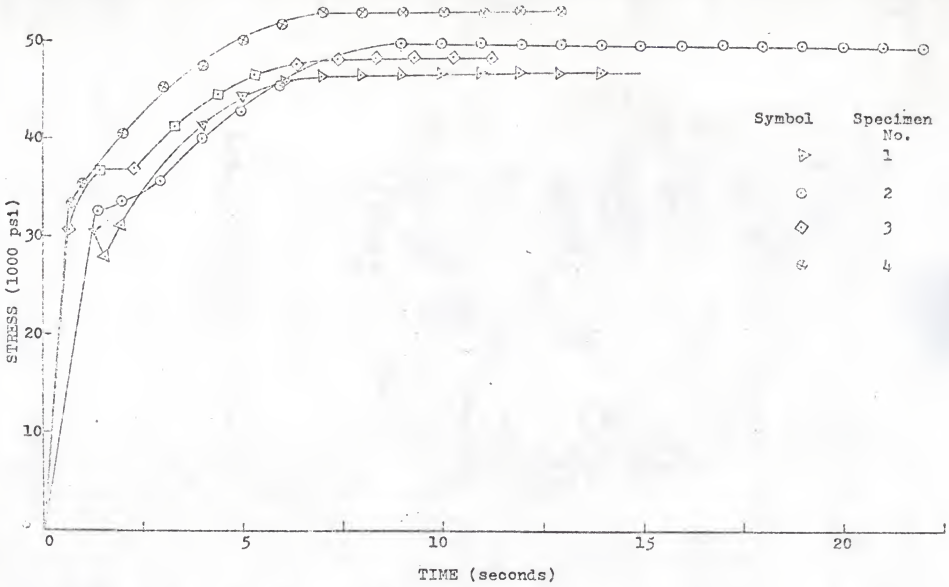

Fig. 27. Stress vs. time diagram obtained for static tests

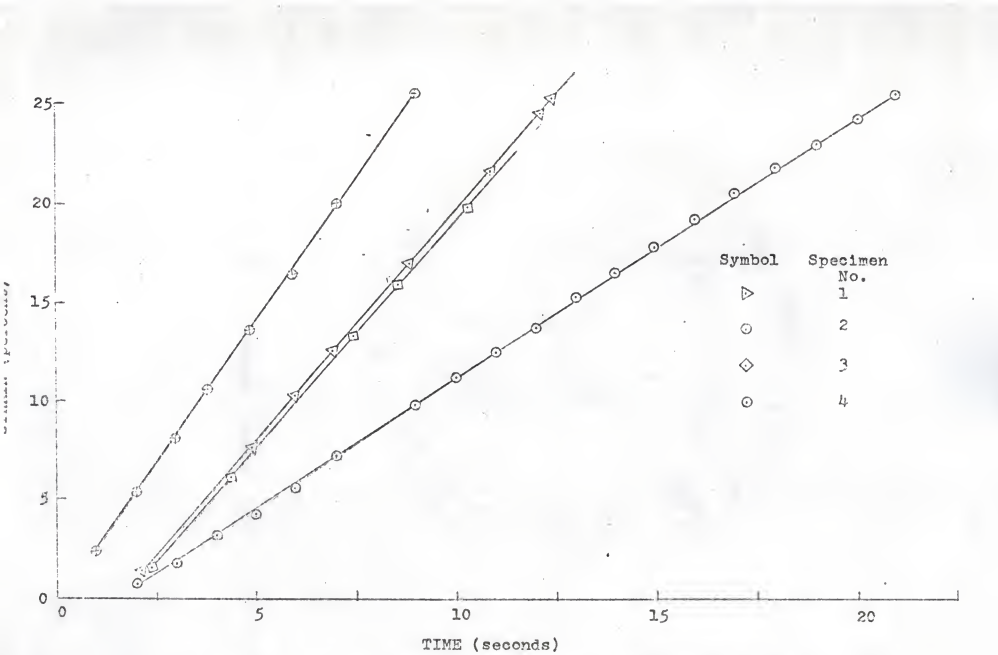

Fig. 28. Strain vs. time diagram obtained for static tests

ACKNOWLEDGEMENTS

The author would like to thank Dr. John C. Lindholm, Major Professor, for his advise and counsel given during the development of work presented in this thesis.

INVESTIGATION OF SOME PROPERTIES OF MILD STEEL AT MODERATE STRAIN RATES

by

NAND SHOWKAT RAI

B. E., University of Jodhpur (India), 1964

AN ABSTRACT OF A MASTER'S THESIS

submitted in partial fulfillment of the

requirements for the degree

MASTER OF SCIENCE

Department of Mechanical Engineering

KANSAS STATE UNIVERSITY
Manhattan, Kansas

1969

Study of behavior of materials at high strain rates is significant first due to the change of stress-strain relationship with strain-rates, second the phenomenon of strain-wave propagation. The effect of strain-wave propagation becomes less significant as strain rates decrease. Since materials during forming processes are subjected to moderate strain rates, it was proposed to determine properties of mild steel at moderate strain rates. To test materials at moderate strain rates without encountering strain wave propagation effects a test fixture was designed and fabricated at Kansas State University. The author used this test fixture to test mild steel (C-1018) tubular specimen in the annealed condition.

This thesis presents the details of experiment performed. Both static and moderate strain rates tests were performed. From experimental results it was concluded that the mild steel is a strain rate sensitive material i.e. yield stress and ultimate stress increase with strain rates. It was also found that yield stress is more strain-rate sensitive than ultimate stress. The results were compared with theory of Campbell [17] who on basis of Theory of Dislocation developed the expression for yield stress as a function of strain rate. On basis of mechanics of plastic deformation a theoretical expression for relationship of stress, strain and strain rate of rigid-plastic material of thin tube was developed.

From test data general relationship between stress-strain at various rates was shown in the form of diagrams. Empirical relation between these quantities could not be established due

to insufficient data available. Certain improvements in both stress and sensing device is desired in order to obtain reliable data at strain rates beyond 15 in./in./sec. Such improvements were suggested. Certain modifications were made in the design of test fixtures to perform the static test on specimen.